Inference of oxygen vacancies in hydrothermal $Na_{0.5}Bi_{0.5}TiO_3$

Aoife O'Brien,[1] David I. Woodward,[1] Kripasindhu Sardar,[2] Richard I. Walton,[2] Pam A. Thomas[1a]
[1]*Department of Physics, University of Warwick, Coventry CV4 7AL, UK.*
[2]*Department of Chemistry, University of Warwick, Coventry CV4 7AL, UK.*
[a)]Author to whom correspondence should be addressed. Electronic mail: p.a.thomas@warwick.ac.uk

Abstract
A high-resolution x-ray powder diffraction study has been made of pseudo-rhombohedral and tetragonal phases in $Na_{0.5}Bi_{0.5}TiO_3$ (NBT), produced via hydrothermal and conventional solid-state methods. Hydrothermal NBT exhibits significantly greater structural distortion at room temperature than solid-state NBT. Peak widths and superstructure peak intensities show a phase transition at ~ 305 °C, with trends suggesting that the structure tends towards cubic symmetry at this temperature. Structural refinements indicate that the transition occurs via a phase coexistence region with no clear intermediate phase. Piezoelectric data show evidence of polarisation pinning in hydrothermal NBT, interpreted as a high proportion of oxygen vacancies.

Text
Sodium bismuth titanate, $Na_{0.5}Bi_{0.5}TiO_3$ (NBT) is a widely-studied relaxor perovskite of potential use as a lead-free piezoelectric, particularly as the end-member of a range of solid solutions including NBT-$BaTiO_3$ and NBT-$K_{0.5}Bi_{0.5}TiO_3$.[1] At room temperature, the structure has long been designated as rhombohedral *R*3*c*,[2] although recent studies have suggested monoclinic *Cc* symmetry for both single crystals[3] and sintered ceramics.[4] However, the deviation from rhombohedral symmetry is very small and the room-temperature structure may be considered pseudo-rhombohedral. On heating, a phase transition to tetragonal symmetry is known to exist, but has been reported to take place over a range of temperatures: 278-291 °C,[5] 240-270 °C[6] and 300-320 °C.[7] At the boundary between pseudo-rhombohedral and tetragonal structures, some studies[8] have shown the existence of a two-phase region, while others[9] have proposed the presence of an intermediate phase. The phase transition to the cubic structure takes place at 500-550 °C[8,10] although some studies[11,12] refer to the pseudo-rhombohedral – tetragonal transition as the ferroelectric Curie temperature.

In this study, the structures, phase transitions and piezoelectric properties of polycrystalline NBT produced by a low-temperature hydrothermal method are investigated and compared with those of a sample made by conventional solid-state synthesis. This study is motivated by the observation over many years that the structures and physical properties of NBT can vary significantly depending on the synthetic method adopted and the thermal history of the material.[4] Limited previous studies of hydrothermal NBT have been undertaken[12,13] but the structural phase transitions and piezoelectric properties of hydrothermal NBT have not been investigated before.

NBT was synthesised in an autoclave with a polytetrafluoroethane liner using a 1:4 molar ratio of Bi_2O_3:TiO_2 (99.9%, Janssen Chimica, α-Bi_2O_3, and >98%, BDH, anatase polymorph, respectively). Typically ~4 g Bi_2O_3 and the corresponding amount of TiO_2 were reacted in a 125 ml autoclave. 60 ml of 10 M NaOH solution was added and the suspension stirred for 2 hours. The autoclave was placed in an oven at 240 °C and left at autogenous pressure for 5 days before cooling. The resulting precipitate was washed with boiling water to remove excess hydroxide, and dried at 70 °C, followed by heating to 950 °C for 6 hours. Heating and cooling rates were 180 °C h^{-1} and 120 °C h^{-1} respectively. NBT was also synthesised via a conventional solid-state reaction, using reagents Na_2CO_3 (99.9%), TiO_2 (99.6%) and Bi_2O_3 (99.975%) (Alfa Aesar) in stoichiometric quantities, which were ball-milled in ethanol for 24 hours and calcined at 900 °C for 6 hours.

X-ray diffraction (XRD) θ-2θ scans were carefully performed in the range of 2θ from 20° to 100° using a Panalytical X'Pert Pro with a curved Johansson monochromator, giving high-resolution diffraction

at the CuKα_1 single wavelength. Variable-temperature data were collected with an Anton Paar HTK1200N furnace. The profile data were refined using the full-pattern Rietveld method using *TOPAS-Academic* V4.1. [14] All peaks are labelled using the pseudocubic setting.

Pellets of both powders were formed under uniaxial pressure of ~75 MPa and sintered for 2 h at 1125 °C. These were prepared for dielectric and piezoelectric measurements by grinding flat and applying silver paint to both faces. Dielectric permittivity and loss were measured using an HP 4192A LF Impedance Analyser at a heating rate of 60 °C h^{-1}. Poling of pellets was performed in silicone oil at room temperature by applying a fixed voltage for 1 minute. Measurements of d_{33} were made for five points on each surface of each pellet using a YE2730A d_{33} meter (APC International, Ltd).

The XRD pattern of hydrothermal NBT at room temperature exhibits peaks that are not visibly split, but a superstructure reflection resulting from antiphase tilting of the oxygen octahedra is visible at 38.5 °2θ, corresponding to Miller indices of type ½{311}, consistent with either rhombohedral *R*3*c* or monoclinic *Cc* structures. Structural refinements in both space groups were performed, the results of which (Table I) show a preference for the monoclinic *Cc* model, as expected.[3,4] Whilst temperature-invariant peak broadening due to instrumental effects and particle size is present in all diffraction patterns collected, there are temperature-dependent contributions, which vary also for different types of plane {*hkl*}, because of the spontaneous ferroelastic strain that is present at all temperatures below the phase transition at 540°C. Thus by analysing the widths of the diffraction peaks as a function of temperature, it is possible to extract the characteristics of the phase transitions, even in the absence of obvious peak splittings. Here, the {110} and {111} peaks are observed to narrow with increasing temperature (Figure 1a) with both peaks reach a minimum width in the range 300-320 °C, clearly indicating that this is a phase transition, in agreement with other studies.[5-7] Whilst the equivalent peak widths from solid-state NBT also show this phase transition (Figure 1b), the overall change in peak widths is significantly smaller than for hydrothermal NBT, which therefore evidences this particular transition much more clearly than has been seen before. The increase in the {110} peak width above this phase transition is consistent with emerging tetragonal symmetry, indicating 300 (10) °C as the pseudo-rhombohedral–tetragonal phase transition temperature, in agreement with optical birefringence measurements.[15] At 300 °C and above, ½{310} superstructure reflections associated with in-phase tilting are observed at 36.5 °2θ, consistent with the tilted tetragonal structure with polar space group *P*4*bm*.[8] The intensities of the weak antiphase and in-phase superstructure reflections were carefully measured using an iterative method after Sonneveld & Visser[16] in PANalytical HighScore Plus[17] and normalised against the most intense reflection. Plotted as a function of temperature (Figure 2a), these show the same trends as the peak widths. The intensities of the superstructure reflections reflect the octahedral tilt angle,[18] showing that the angle of tilt in the pseudo-rhombohedral phase decreases as the phase transition is approached and that the angle of tilt in the tetragonal phase reaches a maximum at 400 °C, in the middle of the tetragonal phase field, consistent with the maximum attained in the width of the {110} peak (Figure 1a) at this same temperature. Superstructure peak intensities from the pseudo-rhombohedral structure are observed to be weaker in solid-state NBT (Figure 2b) although they follow the same trend as those of hydrothermal NBT.

Table I. Lattice parameters and statistics for structures in space groups *R*3*c* (hexagonal setting) and *Cc* refined against XRD data from hydrothermal NBT collected at room temperature.

Space Group	R_{wp} (%)	R_p (%)	χ^2	*a* (Å)	*b* (Å)	*c* (Å)	*β* (°)
Cc	8.7	6.4	1.5	9.5324(2)	5.4833(1)	5.5104(2)	125.417(1)
*R*3*c*	9.6	7.1	1.7	5.4897(2)	*= a*	13.4914(6)	

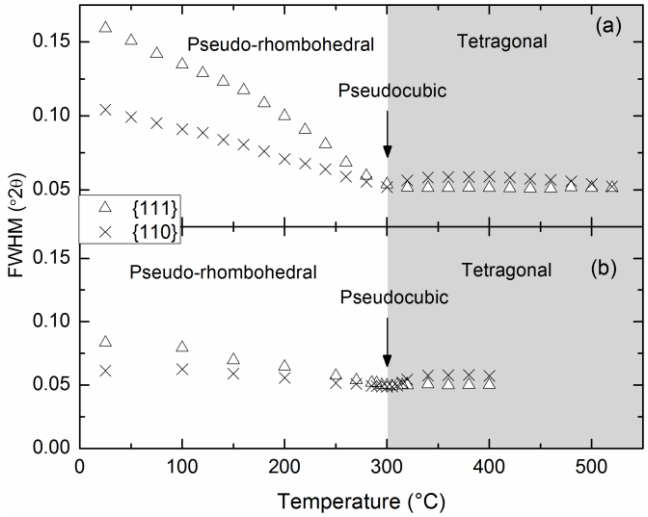

Figure 1. Variation in full width half maximum (FWHM) values of {110} and {111} peaks on heating for (a) hydrothermal and (b) solid-state NBT.

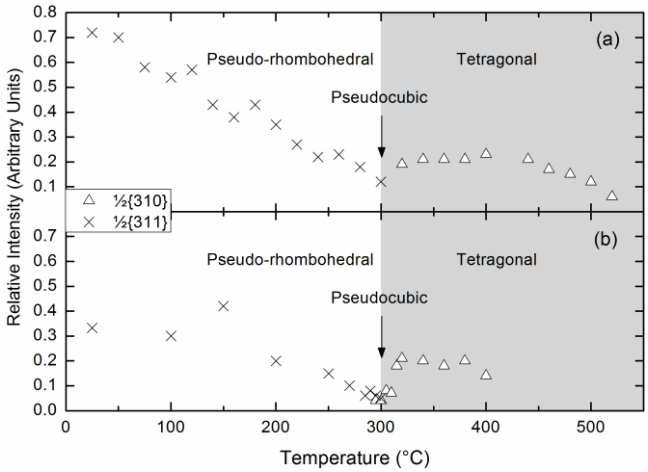

Figure 2. Relative intensities of superstructure reflections in: (a) hydrothermal; (b) solid-state NBT.

Full-pattern XRD data were then acquired over a long scan (13 h) in a wide angular range (20 – 100 °2θ) to focus on the phase transition. At 305 °C, the pattern shows the presence of peaks from both antiphase and in-phase tilting, consistent with phase coexistence or an intermediate phase (Figure 3). Structural refinements carried out against these data show a better fit for phase coexistence than for intermediate phases with the mixed tilt systems required to give both superstructure peaks (space groups *Pnma*, *Cmcm* and $P2_1/m$) (Table II). The best single-phase refinement was in space group *Pnma*; however, this space group would give rise to additional diffraction peaks that are not seen in the pattern. Based on these data, it is concluded that the appearance of both in-phase and antiphase tilt peaks is due to the coexistence of both pseudo-rhombohedral and tetragonal phases. However, the trends in peak widths and superstructure peak intensities indicate that at 305 °C, an untilted cubic structure is approached. The trend in {110} peak widths and superstructure peak intensities in the tetragonal phase is particularly unusual, indicating that tetragonal distortion is maximised in the middle of the phase field, while at both the upper and lower temperatures of the tetragonal regime, it appears that the structure tends towards a metrically cubic phase. The data give no indication of a phase transition at ~200 °C, a temperature associated with depoling of NBT ceramics,[19] confirming that depoling is not associated with a structural phase transition, as also reported by Aksel *et al*.[20]

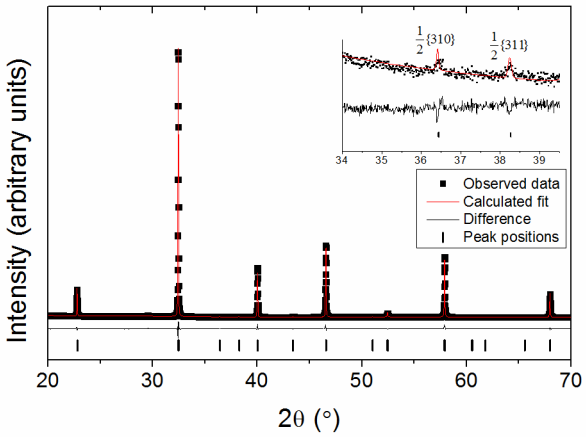

Figure 3. Profile fit to XRD data from hydrothermal NBT at 305 °C. Observed data are given by squares, the calculated model is given as a line with the difference plot below and tick marks indicate the position of peaks. The inset shows the coexistence of both ½{310} in-phase and ½{311} antiphase tilt peaks.

Table II. Lattice parameters and statistics for refinements of hydrothermal NBT at 305 °C in space groups: *Cc*, *P4bm*, *Pnma*, *Cmcm* and $P2_1/m$. The asterix (*) indicates the best fit to the data.

Space Group		R_{wp} (%)	R_p (%)	χ^2	*a* (Å)	*b* (Å)	*c* (Å)	*β* (°)
**R3c/P4bm*	*R3c*	5.6	4.2	1.7	5.5108(1)	= *a*	13.504(2)	
	P4bm				5.50869(2)	= *a*	3.89764(3)	
Cc/P4bm	*Cc*	5.7	4.0	1.7	9.5406(4)	5.5107(1)	5.5130(2)	125.282(4)
	P4bm				5.50961(5)	= *a*	3.89533(7)	
Pnma		6.0	4.4	1.8	5.5085(2)	7.79472(6)	5.5083(2)	
Cmcm		12.1	7.1	3.6	7.78988(5)	= *a*	7.79533(1)	
$P2_1/m$		13.4	7.5	4.0	5.51186(4)	7.79683(5)	5.5249(1)	90.056(3)

Permittivity and loss data acquired for both hydrothermal and solid-state pellets are shown in Figure 4. Both show broadly the same features; a peak in permittivity at ~350 °C, and a shoulder at ~200 °C. The permittivity is lower for the hydrothermal sample and the losses greater for the solid-state sample, particularly at 5 kHz between 200 and 400 °C, but this range of values is normal for NBT, which is known to be particularly sensitive to stoichiometry.[21] The observed difference may therefore correspond to a small difference in stoichiometry. However, the effect of poling on the piezoelectric properties (Figure 5) shows several significant differences between the responses of the two materials. The hydrothermal material has much larger point-to-point variation in the piezoelectric coefficient, d_{33}, resulting in a larger standard deviation of the data. In addition, the d_{33} is not fully reversible; having a mean value of 53 (8) pC/N when initially poled, but a mean value of -35 (4) pC/N when reversed. This is in contrast to solid-state NBT which has d_{33} = 63 (2) pC/N initially and -64 (2) pC/N when reversed. This indicates that polarisation pinning has taken place within hydrothermal NBT. Similar effects have been observed in fatigued ceramics of $Pb(Zr,Ti)O_3$,[22] where it is proposed that accumulation of charges at grain boundaries prevents the switching of individual grains. However, the maximum measurements of d_{33} for the hydrothermal and solid-state samples were 67.7 and 69.0 pC/N, respectively, sufficiently similar values to conclude that the intrinsic physical properties of NBT are unchanged by the synthesis method adopted.

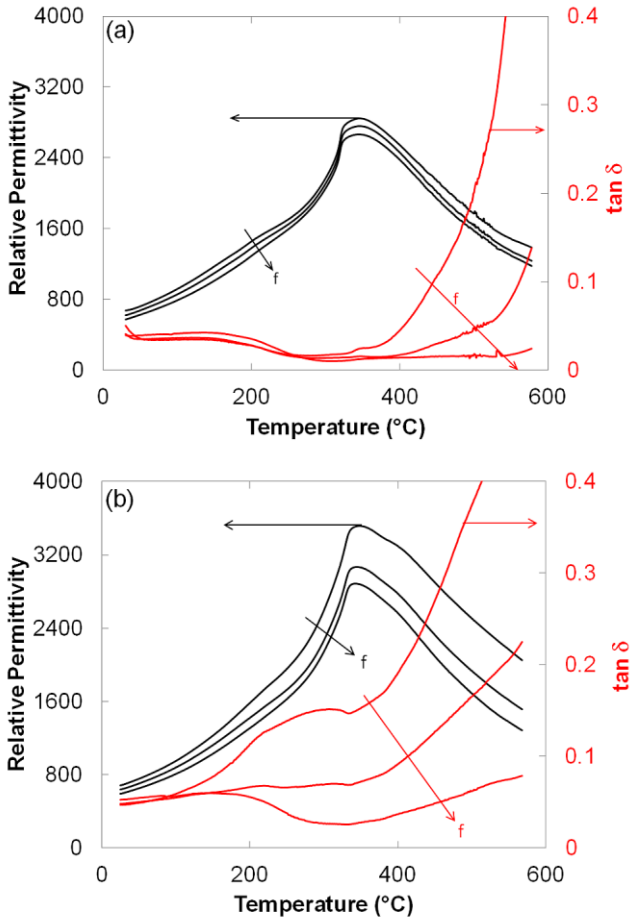

Figure 4. Permittivity data obtained on heating at frequencies 5 kHz, 45 kHz and 505 kHz from (a) hydrothermal NBT, (b) solid-state NBT. Arrows labelled 'f' indicate increasing frequency between data sets.

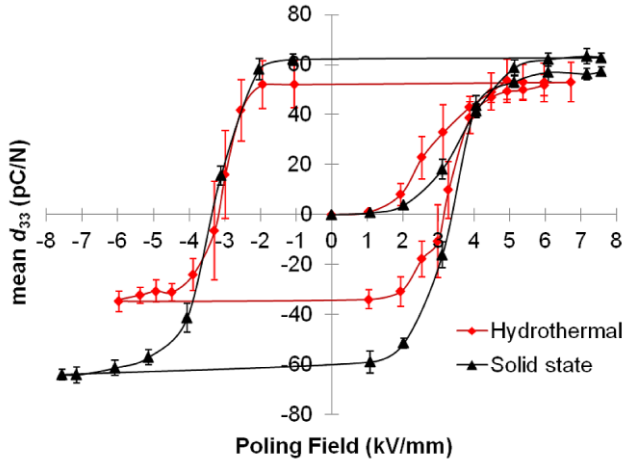

Figure 5. d_{33} as a function of poling field for NBT ceramics made by hydrothermal and solid-state methods.

Calculation of the rhombohedral distortion from refined lattice parameters show that hydrothermal NBT has approximately 1.5 times the spontaneous strain of solid-state NBT at room temperature. In the hydrothermal material, it is possible that OH^- anions may be incorporated into the structure.[13,23] OH^- anions are removed as water by heating above 400 °C,[13] which may generate oxygen vacancies.

It is known that oxygen vacancies accrete on {111} planes in $BaTiO_{3-\delta}$[24] and we therefore propose that the same could occur in NBT to enhance the distortion at room temperature. It is plausible that the resultant material has a higher proportion of vacancies than solid-state NBT, explaining the enhanced structural distortion, the polarisation pinning and, assuming that there is a heterogeneous distribution of these vacancies, the large variation in d_{33}. In contrast, for solid-state samples, cation non-stoichiometry is more likely,[21] which would explain the differences in dielectric loss. Infrared spectroscopy on several hydrothermally-synthesised perovskites (data not shown) features broad absorption peaks centred on 3400 cm^{-1}. These peaks remain present after heating to 60 °C but are not present in sintered hydrothermal material and are therefore consistent with the presence of OH^- anions in the as-prepared material.[25]

In conclusion, it is shown that hydrothermal NBT exhibits a significantly larger spontaneous strain at room temperature than solid-state NBT. In both samples, the phase transition to the tetragonal structure is at ~305 °C on heating and tetragonal distortion initially increases with temperature, reaching a maximum at ~400 °C. Refinements show that pseudo-rhombohedral and tetragonal structures coexist in the region of the phase transition and trends in peak widths and the intensities of superstructure reflections suggest that the structures tend towards cubic at the phase transition. Evidence for polarisation pinning in hydrothermal NBT is observed in piezoelectric data and it is proposed that this and the enhanced strain are due to the presence of oxygen and cation vacancies arising from incorporation of OH^- anions into the structure of the as-synthesised hydrothermal NBT.

Acknowledgements

We thank Jon Davies, Liam Collins-Macintyre and David Walker for materials. The PANalytical MPD diffractometer used in this research was obtained though the Science City Energy Futures Project: Hydrogen Energy, with support from Advantage West Midlands (AWM) and part funded by the European Regional Development Fund (ERDF).

[1]E. Aksel and J. L. Jones, Sensors **10**, 1935 (2010).
[2]S. B. Vakrushev, B. G. Ivanitsky, B. E. Kvyatkovsky, A. N. Maystrenko, R. S. Malysheva, N. M. Okuneva, and N. N. Parfenova, Sov. Phys. Solid State **25**, 1504 (1983).
[3]S. Gorfman and P. A. Thomas, J. Appl. Cryst. **43**, 1409 (2010).
[4]E. Aksel, J. S. Forrester, J. L. Jones, P. A. Thomas, K. Page, and M. R. Suchomel, Appl. Phys. Lett. **98**, 152901 (2011)
[5]F. Cordero, F. Craciun, F. Trequattrini, E. Mercadelli, and C. Galassi, Phys. Rev. B **81**, 144124 (2010).
[6]S. E. Park and S. J. Chung, in *Proceedings of IEEE 9th Symposium on Applied Ferroelectrics* (IEEE, 1994), p. 265.
[7]G. O. Jones and P. A. Thomas, Acta Crystallogr. B **56**, 426 (2000).
[8]G. O. Jones and P. A. Thomas, Acta Crystallogr. B **58**, 168 (2002).
[9]V. Dorcet, G. Trolliard, and P. Boullay, Chem. Mater. **20,** 5061 (2008).
[10]I. G. Siny, C. S. Tu, and V. H. Schmidt, Phys. Rev. B **51,** 5659 (1995).
[11]G. A. Smolenskii, V. A. Isupov, A. I. Agranovskaya, and N. N. Krainik, Sov. Phys. Solid State **2,** 2651 (1961).
[12]M. M. Lencka, M. Oledzka, and R. E. Riman, Chem. Mater. **12**, 1323 (2000).
[13]N. Kumada, Y. Morozumi, Y. Yonesaki, T. Takei, N. Kinomura, and T. Hayashi, J. Ceram. Soc. Japan **116**, 1238 (2008).
[14]A. A. Coelho, *TOPAS-Academic Version 4.1*, (Coelho Software, Brisbane, 2007).
[15]S. Gorfman, A. M. Glazer, Y. Noguchi, M. Miyayama, H. Luo, and P. A. Thomas, J. Appl. Cryst. 45, 444 (2012).
[16]E. J. Sonneveld and J. W. Visser, J. Appl. Cryst. **8**, 1 (1975).

[17]PANalytical B. V., X'Pert HighScore Plus (2008).
[18]A. M. Glazer, Acta Crystallogr. A **31**, 756 (1975).
[19]M. Davies, E. Aksel, and J. L. Jones, J. Am. Ceram. Soc. **94,** 1316 (2011).
[20]E. Aksel, J. S. Forrester, B. Kowalski, J. L. Jones, and P. A. Thomas, Appl. Phys. Lett. **99**, 222901 (2011).
[21]Y. Hiruma, H. Nagata, and T. Takenaka, J. Appl. Phys. **105**, 084112 (2009).
[22]Y. Zhang, I. S. Baturin, E. Aulbach, D. C. Lupascu, A. L. Kholkin, V. Ya. Shur, and J. Rödel, Appl. Phys. Lett. **86**, 012910 (2005).
[23]A. D. Handoko, G. K. L. Goh, and R. X. Chew, CrystEngComm **14**, 421 (2012).
[24]D. I. Woodward, I. M. Reaney, G. Y. Yang, E. C. Dickey, and C. A. Randall, Appl. Phys. Lett. **84**, 4650 (2004).
[25]R. Kota and B. I. Lee, J. Mater. Sci.: Mater. Electron. **18**, 1221 (2007).